



Meteorin-like protein attenuates doxorubicin-induced cardiotoxicity via activating cAMP/PKA/SIRT1 pathway

Can Hu^{a,b,1}, Xin Zhang^{a,b,1}, Peng Song^{a,b}, Yu-Pei Yuan^{a,b}, Chun-Yan Kong^{a,b}, Hai-Ming Wu^{a,b}, Si-Chi Xu^{a,b}, Zhen-Guo Ma^{a,b,**}, Qi-Zhu Tang^{a,b,*}

^a Department of Cardiology, Renmin Hospital of Wuhan University, Wuhan 430060, China

^b Hubei Key Laboratory of Metabolic and Chronic Diseases, Wuhan 430060, China

ARTICLE INFO

Keywords:

Doxorubicin

METRNL

Oxidative stress

Apoptosis

SIRT1

ABSTRACT

Meteorin-like (METRNL) protein is a newly identified myokine that functions to modulate energy expenditure and inflammation in adipose tissue. Herein, we aim to investigate the potential role and molecular basis of METRNL in doxorubicin (DOX)-induced cardiotoxicity. METRNL was found to be abundantly expressed in cardiac muscle under physiological conditions that was decreased upon DOX exposure. Cardiac-specific overexpression of METRNL by adeno-associated virus serotype 9 markedly improved oxidative stress, apoptosis, cardiac dysfunction and survival status in DOX-treated mice. Conversely, knocking down endogenous METRNL by an intramyocardial injection of adenovirus exacerbated DOX-induced cardiotoxicity and death. Meanwhile, METRNL overexpression attenuated, while METRNL silencing promoted oxidative damage and apoptosis in DOX-treated H9C2 cells. Systemic METRNL depletion by a neutralizing antibody aggravated DOX-related cardiac injury and dysfunction in vivo, which were notably alleviated by METRNL overexpression within the cardiomyocytes. Besides, we detected robust METRNL secretion from isolated rodent hearts and cardiomyocytes, but to a less extent in those with DOX treatment. And the beneficial effects of METRNL in H9C2 cells disappeared after the incubation with a METRNL neutralizing antibody. Mechanistically, METRNL activated SIRT1 via the cAMP/PKA pathway, and its antioxidant and antiapoptotic capacities were blocked by SIRT1 deficiency. More importantly, METRNL did not affect the tumor-killing action of DOX in 4T1 breast cancer cells and tumor-bearing mice. Collectively, cardiac-derived METRNL activates SIRT1 via cAMP/PKA signaling axis in an autocrine manner, which ultimately improves DOX-elicited oxidative stress, apoptosis and cardiac dysfunction. Targeting METRNL may provide a novel therapeutic strategy for the prevention of DOX-associated cardiotoxicity.

1. Introduction

Doxorubicin (DOX)-based chemotherapy remains the cornerstone in cancer treatment; however, its clinical application and therapeutic value are evidently impeded by the life-threatening cardiotoxicity that eventually provokes left ventricular dysfunction and congestive heart failure [1]. Uncontrolled reactive oxygen species (ROS) generation is identified as the leading cause of DOX-induced cellular injury and cardiac dysfunction via inducing oxidative damage to the biomacromolecules and activating the downstream proapoptotic pathways [2]. Besides, the heart itself is especially vulnerable to free radicals damage due to the

less active antioxidant network and negligible regenerative capability [3]. Accordingly, previous studies by us and other laboratories determined that restraining oxidative stress and apoptosis were sufficient to ameliorate DOX-related cardiac damage and dysfunction [4–9]. Dexrazoxane is currently the only FDA-approved cardioprotectant for patients with anthracycline chemotherapy [10]. While given the incidence of bone marrow suppression, hepatotoxicity, tumor-killing capacity reduction and secondary malignancies occurrence, developing safe and effective adjuvant therapies to attenuate DOX-induced cardiotoxicity shows great significance.

Physical activity helps to maintain the mitochondrial function and

* Corresponding author. Department of Cardiology, Renmin Hospital of Wuhan University, Hubei Key Laboratory of Metabolic and Chronic Diseases, Wuhan University at Jiefang Road 238, Wuhan 430060, PR China.

** Corresponding author. Department of Cardiology, Renmin Hospital of Wuhan University, Wuhan 430060, China.

E-mail addresses: zhengma@whu.edu.cn (Z.-G. Ma), qztang@whu.edu.cn (Q.-Z. Tang).

¹ These authors contributed equally to this work.

<https://doi.org/10.1016/j.redox.2020.101747>

Received 28 August 2020; Received in revised form 18 September 2020; Accepted 2 October 2020

Available online 7 October 2020

2213-2317/© 2020 The Author(s).

Published by Elsevier B.V. This is an open access article under the CC BY-NC-ND license

(<http://creativecommons.org/licenses/by-nc-nd/4.0/>).

redox homeostasis, and stimulates diverse cardioprotective adaptations to cancer patients with anthracycline chemotherapy [11,12]. Jensen et al. found that exercise preconditioning also decreased DOX accumulation within the heart, thereby preventing cardiac damage and systolic/diastolic impairment [13]. Moreover, exercise does not affect the toxic effects of DOX to cancer cells [14]. Based on the convenience, security and efficiency, aerobic exercise is recommended as a non-pharmacological method to protect against DOX-induced cardiotoxicity [15]. Nevertheless, the physical endurance is obviously decreased in cancer patients due to cachexia, cardiopulmonary dysfunction or other complications [16]. Therefore, understanding the molecular basis and then artificially imitating the beneficial effects of exercise may provide novel insights to mitigate cardiac injury for DOX-treated cancer patients. Myokines are kinds of peptides or cytokines produced by muscle fibres and mediate multiple health benefits of physical activity [17]. They not only modulate systemic metabolism in an endocrine manner, but function as cardioprotectants to prevent pathological remodeling and ischemia-reperfusion injury [18]. Wang et al. demonstrated that the myokine, fibroblast growth factor 21 (FGF21) inhibited oxidative stress and apoptosis, thereby protecting against DOX-induced cardiac injury and dysfunction [19]. Our recent findings also proved that other two myokines, fibronectin type III domain-containing 5 (FNDC5) and osteonin significantly reduced oxidative damage and apoptosis in DOX-treated hearts or cardiomyocytes [4,6]. Besides, Suzuki et al. previously reported that the protective effects against DOX-induced cardiotoxicity of intracoronary myoblasts infusion might be associated with the secretion of a certain bioactive factors [20]. These compelling evidences identify myokines as a promising target to overcome DOX-induced cardiotoxicity, especially for those who cannot tolerate the normal exercise.

Meteorin-like (METRNL) protein is a newly identified myokine that acts to regulate energy expenditure and inflammation in adipose tissue [21–23]. Besides, METRNL is reported to be abundantly expressed in the heart and plays critical roles during the pathogenesis of cardiovascular diseases [21,22]. Liu and colleagues observed that serum METRNL concentrations were decreased in patients with coronary artery disease and also negatively correlated with the Gensini score [24]. A very recent study revealed that METRNL suppressed endoplasmic reticulum stress and apoptosis in H9C2 cells upon oxygen-glucose deprivation and reperfusion stimulation [25]. Herein, we aimed to investigate the potential role and molecular basis of METRNL in DOX-induced cardiotoxicity.

2. Methods

2.1. Reagents and antibodies

DOX, H89, 2',5'-dideoxyadenosine (2',5'-dd-Ado) and brefeldin A (BFA) were purchased from Sigma-Aldrich (St. Louis, MO, USA). Cell counting kit-8 (CCK-8) was obtained from Dōjindo Laboratories (Kumamoto, Japan), while TdT-mediated dUTP nick end-labeling (TUNEL) staining kit was purchased from Millipore (Billerica, MA, USA). The assay kits for silent information regulator 1 (SIRT1) activity, NAD/NADH level, protein kinase A (PKA) activity, cAMP level, catalase (CAT) activity and 3-nitrotyrosine (3-NT) level were obtained from Abcam (Cambridge, UK). Dihydroethidium (DHE), 2',7'-dichlorodihydro fluorescein diacetate (DCFH-DA) and caspase3 activity assay kits were obtained from Beyotime Biotechnology (Shanghai, China). Malondialdehyde (MDA) content, 4-hydroxynonenal (4-HNE) level and total superoxide dismutase (SOD) activity detecting kits were purchased from Nanjing Jiancheng Bioengineering Institute (Nanjing, China). Neutralizing antibody against METRNL and recombinant METRNL protein were obtained from R&D system (Minneapolis, USA). Antibodies against SOD2, heme oxygenase-1 (HO-1), NF-E2-related factor 2 (Nrf2), METRNL and SIRT1 were obtained from Abcam (Cambridge, UK). Anti-B cell lymphoma 2 (BCL-2), anti-BCL-2-associated X protein (BAX) and

anti-glyceraldehyde 3-phosphate dehydrogenase (GAPDH) were purchased from Cell Signaling Technology (Danvers, MA, USA). Proliferating cell nuclear antigen (PCNA) antibody was obtained from Santa Cruz Biotechnology (Dallas, TX, USA).

2.2. Animals and treatments

All animal experiments were approved by the Animal Care and Use Committee of Renmin Hospital of Wuhan University and performed in compliance with the *Guidelines for Care and Use of Laboratory Animals* published by the US National Institutes of Health (NIH Publication No. 85-23, revised 1996). Male C57BL/6 mice (8-10-week-old) were purchased from the Institute of Laboratory Animal Science, Chinese Academy of Medical Science (Beijing, China), and kept in a specific pathogen free barrier system with free access to the standard laboratory chow diet. After acclimation for one week, the mice received a single intravenous injection (1×10^{11} viral genome per mouse) of a cardioprotective adeno-associated virus serotype 9 (AAV9; Hanbio Biotechnology Co., Ltd.; Shanghai, China) carrying *Metrn1* under control of a cTnT promoter to specifically overexpress METRNL in hearts or a negative control AAV9 (*Ctrl*) [4,6]. To knock down endogenous METRNL, the mice were intramyocardially injected with adenoviral vectors (AdV; Hanbio Biotechnology Co., Ltd.; Shanghai, China) containing the short hairpin RNA against *Metrn1* (sh*Metrn1*) or a scramble RNA (shRNA) [26]. Four weeks post-AAV9 or three days after AdV treatment, mice were intraperitoneally injected with DOX (4 mg/kg/week) for consecutive 4 weeks to imitate the cardiotoxicity upon chronic DOX exposure [5]. Mice were then sacrificed for functional and molecular analysis one week after the final DOX treatment, while the survival data were calculated weekly for 9 weeks from the first DOX injection. In neutralizing study, the mice were intraperitoneally injected with a neutralizing antibody (NAb) against METRNL (30 µg/day per mouse, once every two days for consecutive 3 times) or isotype-controlled IgG after the final DOX injection, which then maintained for one week before sacrifice [21]. In another set of experiment, one week after NAb administration, the mice were exposed to a single intravenous injection of AAV9 for additional 4 weeks to replenish cardiac METRNL.

To validate the role of SIRT1, cardiac-restrict *Sirt1* knockout (cKO) mice were constructed as previously described [26]. Briefly, *Sirt1* conditional floxed mice (Provided by X Gao, Nanjing University) were bred with mice carrying the α -Mhc-MerCreMer transgene (Jackson Laboratory) to generate double transgenic mice, while the α -Mhc-MerCreMer transgenic littermates were selected as the control (Con). To delete SIRT1 in cardiomyocytes, the double transgenic mice were intraperitoneally injected with tamoxifen (25 mg/kg/day, dissolved in corn oil) for consecutive 5 days.

2.3. Echocardiography and hemodynamics

Echocardiography was conducted using a MyLab 30CV ultrasound system (Esaote SpA, Genoa, Italy) as previously described [27,28]. Mice were anesthetized by 1.5% isoflurane and then the functional parameters were recorded in a blinded manner. Hemodynamic parameters were collected using a Millar 1.4F catheter transducer (SPR-839; Millar Instruments, Houston, TX) [4,6].

2.4. Cell culture and isolation

H9C2 cell lines were cultured in DMEM medium with 10% fetal bovine serum (FBS) and then serum deprived for 16 h to achieve synchronization. To overexpress METRNL, cells were infected with the adenovirus (DesignGene Biotechnology; Shanghai, China) carrying *Metrn1* (Ad*Metrn1*) or a control vector (Ad*Ctrl*) at a multiplicity of infection of 80. Besides, H9C2 cells were transfected with the small interfering RNA against *Metrn1* (si*Metrn1*, 50 nmol/L) using Lipo 6000™ for 4 h to knock down endogenous METRNL or a scramble RNA (siRNA)

as the negative control [4,5]. Four hours after adenovirus or siRNA treatment, cells were kept in normal medium for additional 24 h to allow gene manipulation. Next, the cells were incubated with DOX (1 $\mu\text{mol/L}$) for 24 h to imitate DOX injury in vitro [4–6]. To neutralize the extracellular METRNL, NAb (1 $\mu\text{g/mL}$) or IgG was added at the same time with DOX. In a separated study, cells were treated with BFA (2.5 $\mu\text{mol/L}$) in serum-free medium for 4 h to block protein secretion after AdMetnrl infection [29]. To verify the involvement of SIRT1, cells were preinfected with siSirt1 (50 nmol/L) or siRNA for 4 h and kept for additional 24 h before AdMetnrl and DOX treatment. Besides, 2'5'-ddAdo (200 $\mu\text{mol/L}$) or H89 (10 $\mu\text{mol/L}$) was used to inhibit cAMP/PKA pathway along with DOX stimulation [30]. For exchange protein directly activated by cAMP (EPAC) silence, cells were pretransfected with siEpac (50 nmol/L) before AdMetnrl infection.

To clarify METRNL secretion from the murine hearts and adult cardiomyocytes, the mouse heart was excised and perfused on a Langendorff apparatus (55 mmHg, 37 °C). The outlet perfusate within 2 h was collected with the first 30 min removed. Then the perfusate samples were centrifuged at 3000 rpm for a total of 45 min (Repeated for 3 times every 15 min). In addition, the adult mice cardiomyocytes (CMs) were isolated by the Langendorff perfusion system as our previously described and cultured in vitro for 4 h with the medium collected to detect METRNL secretion [31]. Cardiac endothelial cells (ECs) were isolated from adult mice using CD31 microbeads, while cardiac fibroblasts (CFs) were isolated using feeder removal microbeads with magnetic cell separation technology as our previously described [26].

2.5. Western blot and quantitative real-time PCR

Total proteins were extracted using RIPA lysis and the nuclear proteins were prepared by a commercial kit as our previously described [7, 27, 32]. Then the isolated proteins were separated with sodium dodecyl sulfate polyacrylamide gels and transferred onto polyvinylidene fluoride membranes. Next, the membranes were blocked with 5% skim milk (Room temperature, 1 h) and probed with the primary antibodies (4 °C, overnight), followed by the incubation with secondary antibodies at room temperature for additional 1 h. Protein bands were visualized by the ECL reagent using a ChemiDoc™ XRS + system and analyzed using an Image Lab software (Bio-Rad Laboratories, Inc.). Total RNA was isolated by a TRIzol reagent and transcribed to cDNA by the Maxima First Strand cDNA Synthesis Kit (Roche; Basel, Switzerland). Quantification was performed on the Roche LightCycler® 480 detection system and normalized to *Gapdh* [7, 30].

2.6. Intracellular ROS detection

Intracellular ROS production was detected by DHE staining in vivo and DCFH-DA staining in vitro as our previously described [5, 6]. Frozen heart sections were stained with DHE (5 $\mu\text{mol/L}$), while H9C2 cells were incubated with DCFH-DA (5 $\mu\text{mol/L}$) at 37 °C for 30 min in the dark. The images were captured using a fluorescence microscope (Olympus; Tokyo, Japan) in a blinded manner.

2.7. Immunofluorescence and TUNEL staining

Nrf2 localization in H9C2 cells was determined by immunofluorescence staining [26, 28]. Briefly, cell coverslips were fixed with 4% paraformaldehyde for 15 min and permeabilized in 1% Triton X-100 for 5 min at room temperature respectively. After blocking with 10% goat serum, the cells were stained with anti-Nrf2 (1:100 dilution) at 4 °C overnight, followed by the incubation with Alexa Fluor®568-conjugated secondary antibodies at 37 °C for 1 h. Finally, the cell nuclei were probed by DAPI and the fluorescence images were recorded by a fluorescence microscope in a blinded manner. TUNEL staining in cardiac sections and cell coverslips was performed using a commercial kit as our previously described [4, 6, 7]. Cell apoptosis was calculated as the ratio

of TUNEL-positive nuclei to DAPI-stained nuclei in six images per heart.

2.8. Biochemical analysis

Serum levels of cardiac injury markers (Lactate dehydrogenase, LDH; cardiac isoform of troponin T, cTnT; creatine kinase isoenzymes, CK-MB) and hepatotoxic biomarkers (Alanine transaminase, ALT; aspartate transaminase, AST) were measured with an ADVIA® 2400 automatic biochemical analyzer (Siemens Ltd.; Tarrytown, NY, USA) [4–6]. The levels of 3-NT (A marker for protein peroxidation), MDA, 4-HNE (Two lipid peroxidation products), LDH releases, NAD⁺, cAMP and the activities for total SOD, CAT, SIRT1, PKA and caspase3 in heart samples or cells were detected by the commercial kits according to the manufacturer's instructions. The concentrations of METRNL in cardiac homogenates, perfusate and medium were measured by enzyme-linked immunosorbent assay (ELISA) methods. Cell viability was assessed using the CCK-8 kit according to our previous studies [4–6].

2.9. Tumor studies in vitro and in vivo

DOX-sensitive 4T1 breast cancer cells were kindly provided by Dr. Q Yang (Renmin hospital of Wuhan University) and cultured in RPMI 1640 medium supplemented with 15% FBS. To investigate the effect of METRNL on the tumor-killing action of DOX, 4T1 cells were incubated with recombinant METRNL protein (0, 50 and 500 ng/mL) in the presence of DOX (1 $\mu\text{mol/L}$) for indicating times [21]. In addition, we also constructed tumor-bearing mice to evaluate the influence of METRNL on DOX chemotherapeutic capacity in vivo [33]. Briefly, the female BALB/c athymic nude mice (4-week-old) received injections of 1×10^6 4T1 cells at the right mammary fat pad and then were exposed to intraperitoneal injections of recombinant METRNL protein (10 mg/kg/day for 3 weeks) together with DOX (4 mg/kg/week for 4 times). One week after the final DOX treatment, mice were sacrificed for the analysis of cardiac function and tumor parameters, while the survival rate was calculated weekly for 7 weeks from the first DOX injection. Tumor diameters were recorded twice a week and calculated using the following formula: tumor volume = $1/2 \times \text{length} \times \text{width} \times \text{height}$. In another set of experiment, the control tumor-bearing mice were infused with recombinant METRNL protein (10 mg/kg/day for 3 weeks) or vehicle, and the serum concentrations of ALT and AST were analyzed one week after the final METRNL injection to determine the hepatotoxic effects.

2.10. Statistical analysis

Data in this study were presented as mean \pm standard deviation (SD) and analyzed by SPSS 22.0 software. The differences between two groups were assessed by an unpaired Student's *t*-test, while differences among three or more groups were compared using the one-way analysis of variance (ANOVA) analysis followed by Tukey post-hoc test. Survival data were analyzed by the Kaplan-Meier method followed with a Mantel-Cox log rank test. A *P* value less than 0.05 was considered statistically significant.

3. Results

3.1. METRNL is downregulated in hearts and cardiomyocytes upon DOX stimulation

We first compared the METRNL abundance across different tissues and detected a higher *Metnrl* mRNA expression in cardiac muscle than that in skeletal muscle or adipose tissue, the two predominant origins of METRNL in previous studies (Fig. 1A) [21, 22]. However, cardiac *Metnrl* mRNA was significantly decreased by DOX injection, accompanied with a slight reduction in skeletal muscle (Fig. 1A). Western blot and ELISA data further confirmed that DOX treatment suppressed METRNL expression in murine hearts (Fig. 1B and C). Besides, *Metnrl* mRNA level

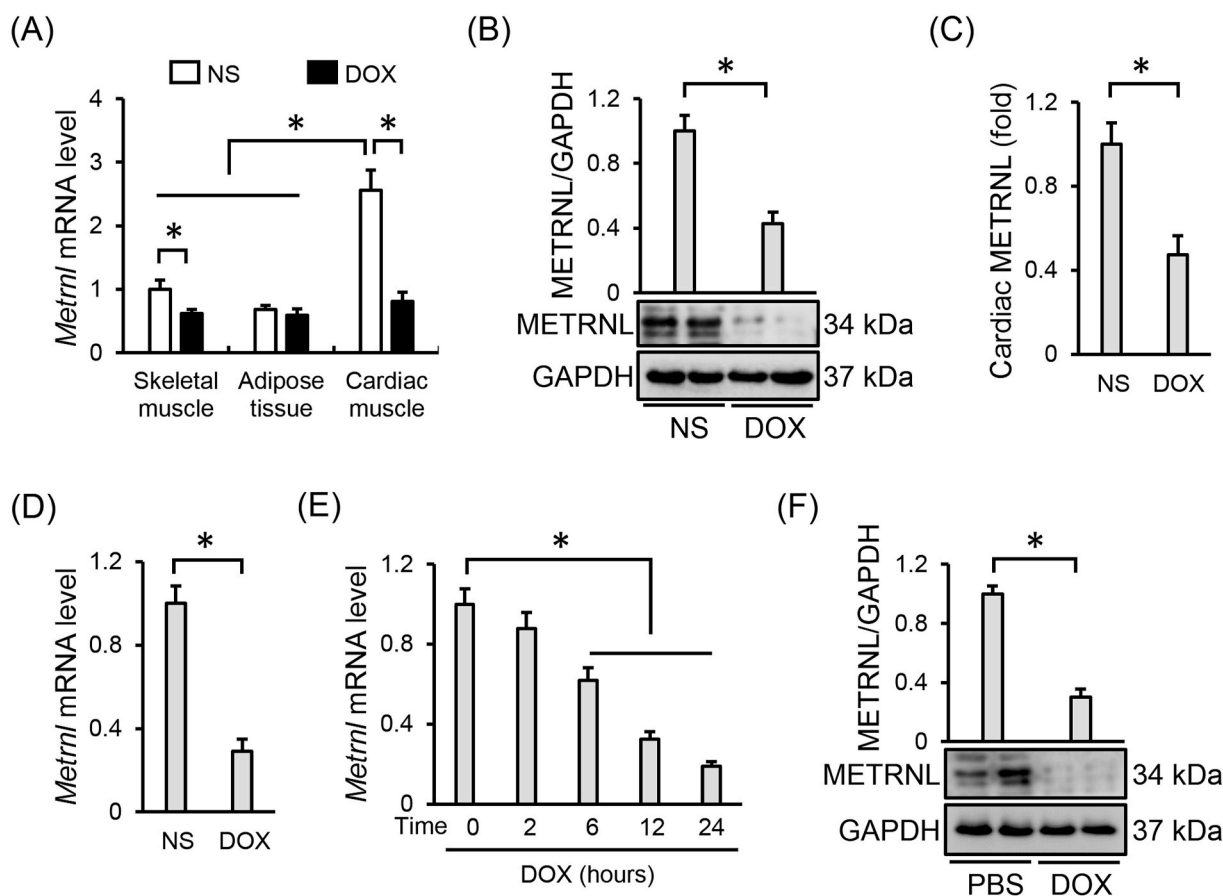


Fig. 1. METRNL is downregulated in hearts and cardiomyocytes upon DOX stimulation. (A) Relative mRNA levels of METRNL in different mouse tissues under DOX treatment (n = 6). (B–C) Cardiac METRNL expression detected by Western blot and ELISA (n = 6). (D) Relative *Metrn1* mRNA level in the adult mouse cardiomyocytes isolated from the hearts with or without DOX treatment (n = 6). (E) Relative *Metrn1* mRNA level in H9C2 cells under DOX stimulation with different times (n = 6). (F) METRNL protein alteration in H9C2 cells after DOX incubation for 24 h (n = 6). Values represent the mean \pm SD. **P* < 0.05 versus the matched group.

was also decreased in the adult cardiomyocytes isolated from DOX-treated mice (Fig. 1D). Accordingly, DOX stimulation inhibited METRNL expression in H9C2 cells, as evidenced by the reduced mRNA and protein levels (Fig. 1E and F).

3.2. METRNL overexpression alleviates DOX-induced cardiotoxicity in mice

To investigate the role of METRNL in DOX-induced cardiotoxicity, mice with AAV9 injection were exposed to repeated DOX treatments to mimic the clinical cardiotoxic effects (Fig. 2A). As shown in Figs. S1A–B, AAV9 injection caused a robust and persistent expression of METRNL in the adult murine hearts and cardiomyocytes. DOX administration induced severe cardiac injury in mice, as verified by the increased serum levels of LDH, cTnT and CK-MB and cardiac *Anp* and *Bnp* mRNA levels, which were all decreased in mice with METRNL overexpression (Fig. 2B and Fig. S1C). Correspondingly, METRNL overexpression markedly preserved fractional shortening (FS) and the peak rates of isovolumic pressure development and pressure decay (\pm dP/dt) in left ventricles upon DOX insult (Fig. 2C–E). Meanwhile, the decreased ratio of heart weight to tibia length (HW/TL) was also prevented by METRNL (Fig. 2F). More importantly, the survival rate was higher in mice with METRNL overexpression after DOX treatment (Fig. 2G). However, no change in food intake or water consumption was observed in mice by METRNL overexpression (Fig. S1D).

3.3. METRNL overexpression inhibits oxidative stress and apoptosis in DOX-treated hearts

Oxidative stress and apoptosis contribute to the development of DOX-related cardiac injury [2]. As shown in Fig. 3A, DOX injection notably increased cardiac ROS generation that was decreased by METRNL replenishment. Excessive free radicals cause protein/lipid peroxidation, and eventually provoke oxidative damage and cell apoptosis [2,4]. Herein, we observed increased levels of biomarkers related to protein (3-NT) and lipid (MDA and 4-HNE) peroxidation in DOX-treated hearts, but to a less extent in those with METRNL overexpression (Fig. 3B and C). Besides, the activities of SOD and CAT, the two important antioxidant enzymes, were inhibited in DOX-stimulated hearts, but increased after METRNL overexpression (Fig. 3D). Nrf2 acts as a critical transcription factor to maintain redox homeostasis [34]. We found that METRNL overexpression restored Nrf2 protein level and nuclear accumulation in hearts with DOX treatment, and that the downstream HO-1 and SOD2 protein levels were also preserved (Fig. 3E–G). TUNEL staining labels DNA breakpoints with 3'-OH terminals that is well-accepted to detect DNA damage and cell apoptosis [35]. As shown in Fig. 4A and B, DOX increased DNA fragmentation and cell apoptosis in the hearts, which were significantly inhibited by METRNL overexpression. As expected, METRNL increased BCL-2 protein abundance, and decreased BAX expression and caspase3 activity in hearts with DOX stimulation (Fig. 4C–E).

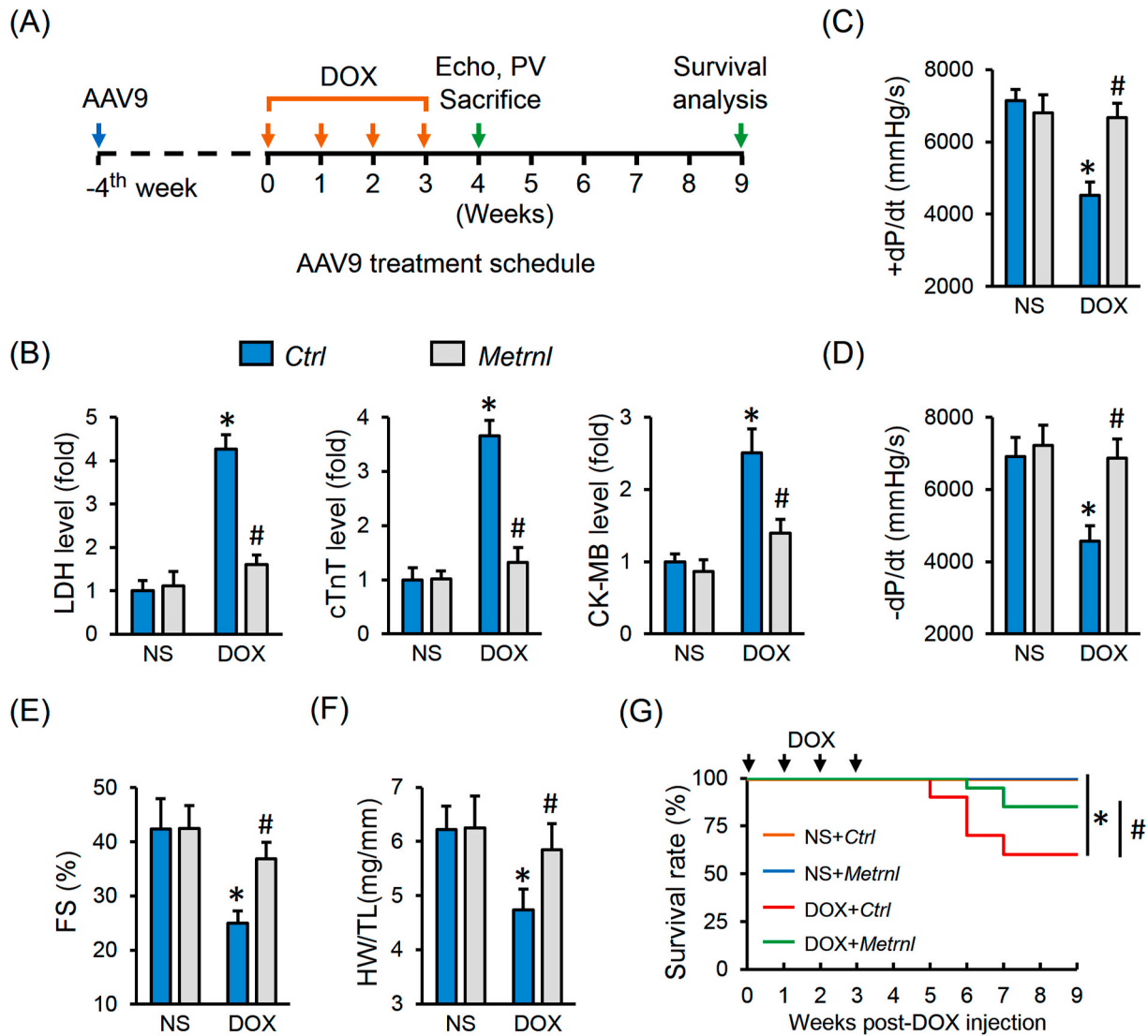


Fig. 2. METRNL overexpression alleviates DOX-induced cardiotoxicity in mice. (A) Schematic protocol for AAV9 and DOX treatment. (B) Serum levels of LDH, cTnT and CK-MB in mice with or without METRNL overexpression after DOX injection ($n = 8$). (C–E) Hemodynamic and echocardiographic parameters of cardiac function ($n = 8$). (F) Statistical data of HW/TL ($n = 8$). (G) The survival curves up to 9 weeks after the first DOX injection in mice with or without METRNL overexpression ($n = 20$). Values represent the mean \pm SD. * $P < 0.05$ versus NS + Ctrl, # $P < 0.05$ versus DOX + Ctrl.

3.4. METRNL deficiency exacerbates DOX-induced cardiac injury and dysfunction in mice

Mice with AdV injection received DOX treatment to explore whether METRNL deficiency aggravated DOX-induced cardiac injury and dysfunction (Fig. S2A). As shown in Figs. S2B–C, AdV injection significantly reduced endogenous METRNL expression in DOX-treated murine hearts. Hemodynamic and echocardiographic data indicated that DOX-elicited cardiac impairment was aggravated by METRNL knockdown (Figs. S2D–E). Meanwhile, METRNL-deficient mice had further decreased HW/TL and elevated serum levels of LDH, cTnT and CK-MB upon DOX injection (Figs. S2F–G). Besides, METRNL silence also increased the mortality rate in DOX-treated mice (Fig. S2H). Further findings revealed that METRNL knockdown promoted intramyocardial ROS production and oxidative damage upon DOX stimulation (Figs. S3A–C). Nrf2 protein abundance and nuclear accumulation as well as the downstream HO-1, SOD2 expression were all decreased in METRNL-deficient hearts (Figs. S3D–F). Accordingly, total SOD and CAT activities in heart samples were inhibited by METRNL knockdown (Fig. S3G). In addition, METRNL silence increased BAX expression and

caspase3 activity, while decreased BCL-2 level, thereby exacerbating DNA damage and cell apoptosis in DOX-injured hearts (Fig. S3H–L). However, METRNL expression pattern, either overexpression or knockdown, did not affect oxidative stress, apoptosis and cardiac function under basal conditions.

3.5. METRNL modulates DOX-induced oxidative damage and apoptosis in vitro

In line with the in vivo data, DOX-triggered decreases of Nrf2, HO-1, SOD2, BCL-2 expression and increases of BAX expression, caspase3 activity were prevented in AdMetrnl-infected H9C2 cells (Figs. S4A–D). Further studies implied that METRNL overexpression suppressed Nrf2 nuclear export and the reduction of antioxidant enzymatic activities upon DOX stimulation (Figs. S4E–F). DCFH-DA and TUNEL staining identified a decreased intracellular ROS generation, DNA fragmentation and cell apoptosis after METRNL overexpression (Fig. S4G). Accordingly, the increased MDA and 3-NT production and decreased cell viability were ameliorated in AdMetrnl-infected cells (Figs. S4H–I). The efficiency of AdMetrnl was determined by PCR analysis (Fig. S4J). In

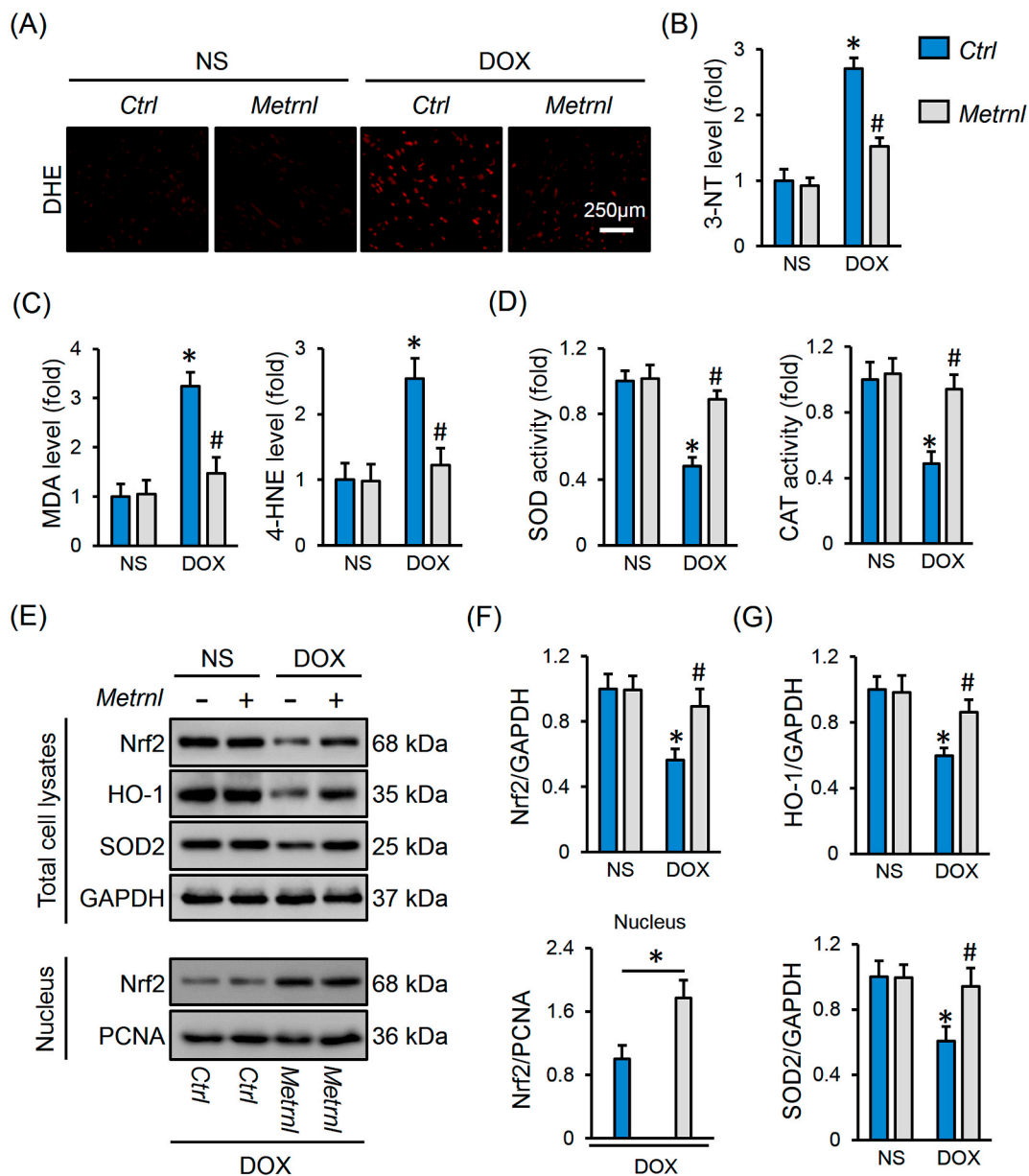


Fig. 3. METRNL overexpression inhibits oxidative stress in DOX-treated hearts. (A) Representative images of DHE staining in heart samples (n = 6). (B–C) The levels of 3-NT, MDA and 4-HNE in heart samples (n = 6–8). (D) Total SOD and CAT activities in hearts (n = 8). (E–G) Representative Western blot images and statistical results (n = 6). Values represent the mean \pm SD. * $P < 0.05$ versus NS + Ctrl, # $P < 0.05$ versus DOX + Ctrl. In Fig. 3F, * $P < 0.05$ versus the matched group.

contrast, METRNL silencing aggravated oxidative damage and apoptosis in H9C2 cells upon DOX incubation (Figs. S5A–G).

3.6. Cardiac-derived METRNL prevents DOX-induced cardiotoxicity in an autocrine manner

We next employed a commercial NAb against METRNL to block its systemic action. As depicted in Figs. S6A–C, NAb injection exacerbated DOX-induced oxidative stress, DNA damage and apoptosis. Cardiac impairment in DOX-treated mice was further compromised by blocking the endogenous METRNL (Fig. 5A). Many tissues can express and secrete METRNL, we thus overexpressed METRNL in cardiomyocytes using cardiotropic AAV9 vectors to verify the role of cardiac-derived METRNL in DOX-induced cardiac injury and dysfunction (Fig. 5B and Fig. S1B). Intriguingly, METRNL overexpression in cardiomyocytes is sufficient to attenuate DOX-induced cardiac dysfunction, accompanied by the decreases of cardiac injury markers (Fig. 5C–D and Fig. S6D). Previous

studies proved that METRNL could be released into the extracellular fluid by skeletal muscle cells and adipocytes [21,22]. In the above study, we detected robust METRNL expression in cardiac muscle and cardiomyocytes; however, it remains unclear whether METRNL is secreted by the cardiomyocytes. Herein, we measured substantial METRNL releases from the isolated murine hearts under Langendorff perfusion, adult mouse cardiomyocytes and H9C2 cell lines (Figs. S6E–F and Fig. 5E). To clarify whether METRNL release is a result of passive leakage, we treated H9C2 cells with BFA and found that the robust METRNL levels in the medium from AdMetrnl-infected H9C2 cells were decreased by BFA incubation (Fig. 5F). Besides, METRNL secretion from the cardiomyocytes was suppressed by DOX treatment (Fig. 5E and Figs. S6E–F). We next used NAb to block the action of extracellular METRNL and found the protective effects of METRNL overexpression were abrogated in H9C2 cells with NAb cotreatment (Fig. 5G–H and Fig. S6G).

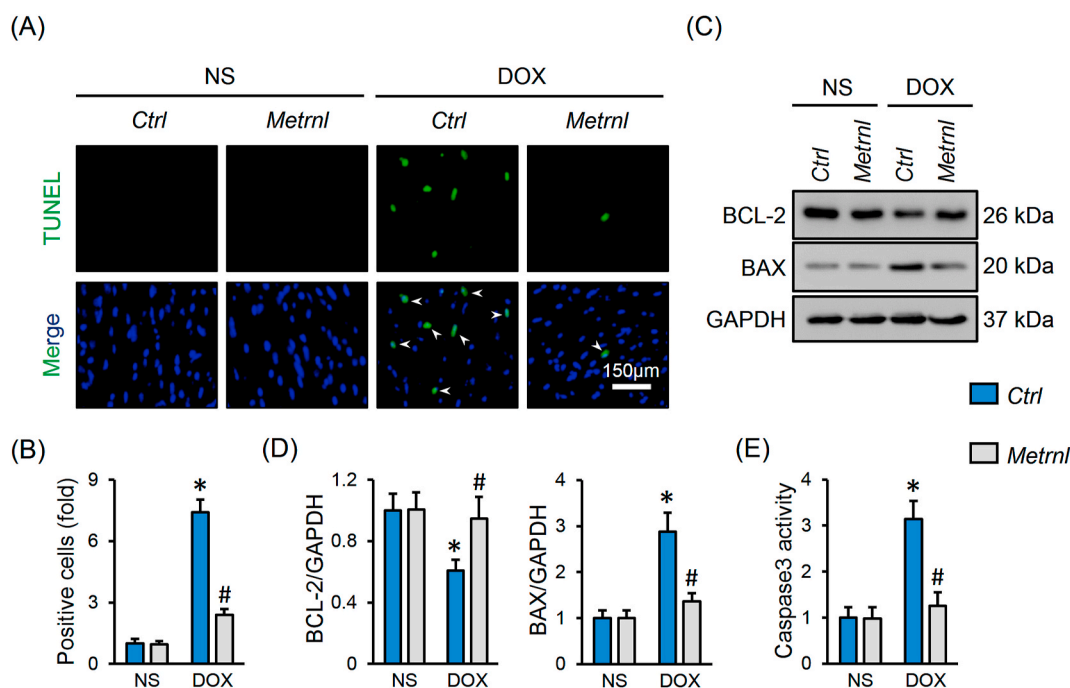


Fig. 4. METRNL overexpression inhibits apoptosis in DOX-treated hearts. (A–B) Representative images of TUNEL staining and the quantitative data about TUNEL-positive nuclei in heart samples ($n = 8$). White arrows indicate TUNEL-positive nuclei. (C–D) Representative Western blot images and statistical results ($n = 6$). (E) Caspase3 activity in heart samples ($n = 8$). Values represent the mean \pm SD. * $P < 0.05$ versus NS + Ctrl, # $P < 0.05$ versus DOX + Ctrl.

3.7. METRNL exerts the cardioprotective effects via activating SIRT1 in vitro and in vivo

SIRT1 is identified as an important cardioprotective molecule and plays vital roles in regulating oxidative stress and apoptosis [36,37]. Previous studies by us and other laboratories proved that SIRT1 activation remarkably alleviated DOX-induced cardiac injury and dysfunction [8,19]. As show in Figs. S7A–D, DOX significantly decreased SIRT1 protein abundance and activity in H9C2 cells that were restored by METRNL overexpression, but further inhibited by METRNL knockdown. To validate the necessity of SIRT1, H9C2 cells were preincubated with siSirt1 and the transfection efficiency was verified in Fig. S7E. The inhibitory effects of METRNL on DOX-induced oxidative damage and apoptosis were negated by SIRT1 silence (Figs. S7F–H). Consistent with the in vitro data, the reduced SIRT1 expression and activity in DOX-treated hearts were preserved by METRNL overexpression (Fig. 6A and B). To further confirm the role of SIRT1 in vivo, cardiac-specific Sirt1 knockout mice were used (Fig. S7I). As depicted in Fig. 6C and D, METRNL overexpression prevented DOX-induced oxidative stress and apoptosis in control hearts, yet failed to do so in cKO mice. Correspondingly, the improved cardiac injury and function by METRNL were completely abolished in SIRT1-deficient hearts (Fig. 6E–G).

3.8. METRNL activates SIRT1 via cAMP/PKA signaling axis

In the above study, we determined increases of SIRT1 protein and activity by METRNL. SIRT1 is a well-known NAD⁺ dependent deacetylase and its activation not only involves an upregulation of protein abundance but also relies on the increase of NAD⁺ concentrations. Interestingly, no alteration of NAD⁺ levels in DOX-treated hearts or H9C2 cells was observed after METRNL overexpression (Fig. S8A). The above findings have proved that METRNL protected against DOX-induced oxidative stress and apoptosis through an autocrine manner, while the second messengers are required for the transmission of extracellular signals to intracellular molecular network. The cAMP acts as an important second messenger and is proved to activate SIRT1 via NAD⁺ independent manners [38,39]. We thus detected cAMP levels,

and found METRNL increased cAMP abundance in DOX-treated hearts and H9C2 cells, accompanied by an activation of PKA (Figs. S8B–C). In addition to PKA, EPAC is the other well-designated downstream effector of cAMP pathway [30]. As indicated in Fig. S8D, SIRT1 activation by METRNL was blunted in H9C2 cells with 2'5'-dd-Ado or H89 treatment, but not in siEpac-transfected cells. Accordingly, the antioxidant and antiapoptotic effects of METRNL were blocked by cAMP/PKA inhibition, yet preserved in cells with EPAC knockdown (Figs. S8E–H).

3.9. METRNL does not affect the tumor-killing capacity of DOX

To evaluate the therapeutic potential of METRNL in the context of DOX therapy, 4T1 breast cancer cells were incubated with DOX and recombinant METRNL protein. As shown in Fig. S9A, METRNL did not affect the tumor-killing action of DOX. In addition, we also constructed tumor-bearing mice to investigate whether METRNL interfered with the chemotherapeutic capacity of DOX (Fig. S9B). DOX-treated BALB/c nude mice with recombinant METRNL protein injections had increased serum and cardiac METRNL levels (Fig. S9C). As expected, DOX treatment delayed tumor growth in vehicle-treated mice, while no significance in tumor volume or weight was observed between DOX + Vehicle and DOX + METRNL groups (Figs. S9D–E). Nonetheless, the compromised cardiac function and increased mortality rate after DOX injection were prevented by METRNL infusion, and no hepatotoxic effect of METRNL was observed during the treatment (Figs. S9F–I).

4. Discussion

DOX shows a high affinity to the heart and is especially retained in the mitochondrial inner membrane due to the formation of a nearly-irreversible complex with cardiolipin. The DOX-cardiolipin complexes not only interfere with the normal electron transport chain to increase free radicals production, but also provoke apoptotic programs given the fact that cardiolipin is important to maintain mitochondrial membrane potential and also serves as an anchor point for cytochrome c to prevent its cytoplasmic leakage [40]. Besides, DOX-derived reactive semi-quinone free radicals during the redox cycling process in turn accelerate

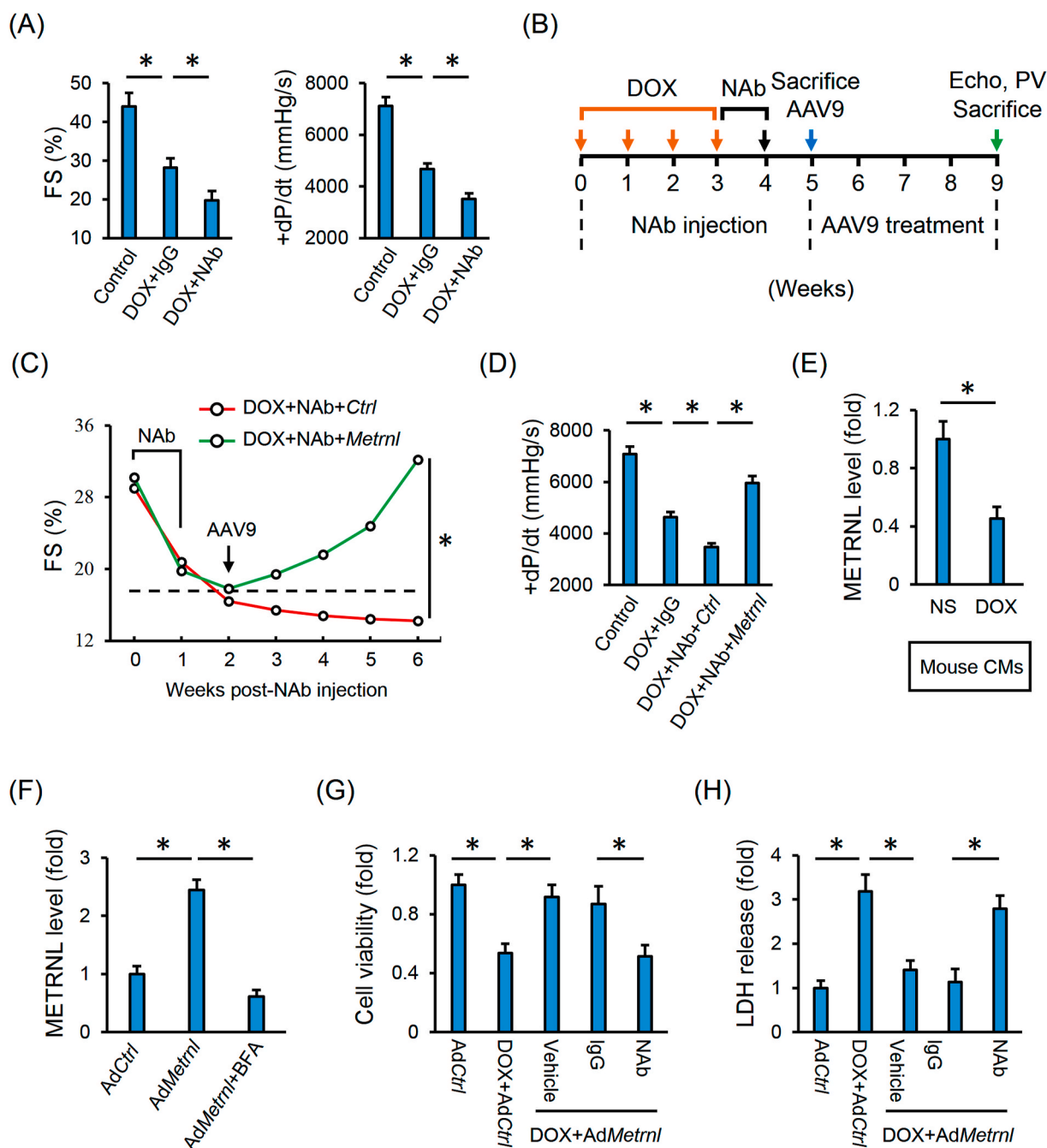


Fig. 5. Cardiac-derived METRNL prevents DOX-induced cardiotoxicity in an autocrine manner. (A) Hemodynamic and echocardiographic parameters of cardiac function in mice with or without NAb injection (n = 5). (B) Schematic protocol for NAb, DOX and AAV9 treatment. (C–D) Hemodynamic and echocardiographic parameters of cardiac function (n = 5). (E) Adult mouse CMs were isolated from the mice with or without DOX injection and then incubated in serum-free medium for additional 4 h to detect METRNL secretion (n = 6). (F) H9C2 cells were infected with the adenovirus and cultured in normal medium for 24 h to allow gene manipulation, which were then treated with BFA (2.5 μmol/L) in serum-free medium for additional 4 h to detect METRNL secretion (n = 6). (G) Cell viability analysis by CCK-8 method (n = 8). (H) LDH release in H9C2 cells (n = 6). Values represent the mean ± SD. **P* < 0.05 versus the matched group.

superoxide anions generation [2]. The increased mitochondrial iron accumulation by DOX treatment also amplifies ROS synthesis through a Fenton-type reaction [41]. Excessive free radicals directly trigger oxidative damage to the cardiomyocytes and motivate intracellular proapoptotic pathways, thereby causing cardiac injury and dysfunction. Nrf2 functions as a redox-sensitive transcription factor and is sequestered in the cytoplasm by Keap 1, which in turn translocates into the nucleus to initiate the transcription of multiple antioxidant genes when challenged with oxidative stress [34]. Consistently, cardiac Nrf2 expression and transcription activity were found to be decreased upon

DOX treatment, but prevented by FNDC5 overexpression, accompanied with an amelioration of oxidative damage and cardiac dysfunction in our previous study [4]. Herein, METRNL also increased cardiac Nrf2 protein abundance and nuclear accumulation, thereby activating the downstream antioxidant enzymes and attenuating DOX-induced cardiac impairment.

SIRT1 is a NAD⁺ dependent histone deacetylase and plays indispensable roles in multiple pathophysiological processes, ranging from cell proliferation, differentiation, migration, aging to death [42]. Matsui et al. found that SIRT1 overexpression notably increased Nrf2 expression

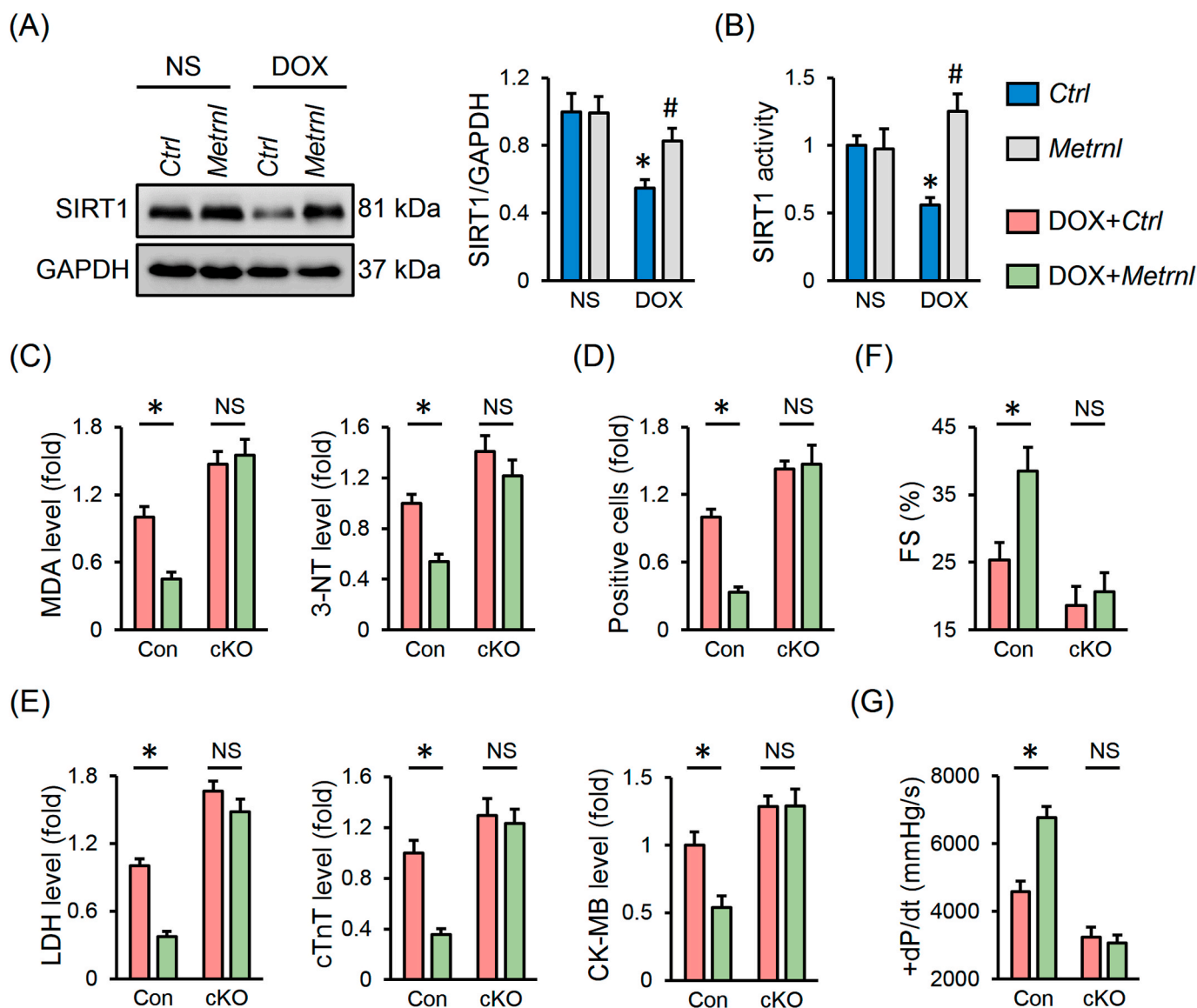


Fig. 6. METRNL exerts the cardioprotective effects via activating SIRT1 in vivo. (A) Cardiac SIRT1 protein abundance and statistical results ($n = 6$). (B) Cardiac SIRT1 activity ($n = 8$). (C) The levels of MDA and 3-NT in heart samples ($n = 6-8$). (D) Quantification of RUNEL-positive nuclei in heart tissues ($n = 8$). (E) Serum levels of LDH, cTnT and CK-MB in mice ($n = 8$). (F-G) Hemodynamic and echocardiographic parameters ($n = 8$). Values represent the mean \pm SD. * $P < 0.05$ versus the matched group. In Fig. 6A and B, * $P < 0.05$ versus NS + Ctrl, # $P < 0.05$ versus DOX + Ctrl. NS indicates no significance.

and nuclear translocation, thereby amplifying the endogenous antioxidant capacity [43]. Besides, SIRT1 also promoted FoxO activation and then upregulated SOD2 transcription [36]. As expected, Wang et al. reported that FGF21 enhanced Nrf2 transcription activity and reduced cardiac ROS generation via SIRT1, while SIRT1 silence abolished this antioxidant effect [19]. Additionally, SIRT1 activation causes p53 deacetylation and subsequently decreases cell apoptosis, in contrast, inhibiting SIRT1 augments p53 activity and apoptosis. Results from Zhang et al. revealed that SIRT1 activation by resveratrol reduced p53 acetylation and apoptosis in DOX-injured hearts [44]. Our previous findings also determined the antiapoptotic and cardioprotective effects of SIRT1 against DOX-induced cardiotoxicity [8]. We herein showed that METRNL activated SIRT1 and then protected the heart from DOX-induced oxidative stress and apoptosis. However, relatively little is known about how METRNL activates SIRT1. Despite the increases of SIRT1 protein abundance by METRNL, its activation also relies on NAD⁺. Unexpectedly, we did not observe any changes of intracellular NAD⁺ levels after METRNL overexpression. METRNL is a secretory myokine and its cardioprotective effects were blocked after neutralizing

the extracellular action. Second messengers are required for the transmission of extracellular signals to intracellular molecular network and cAMP acts as an important second messenger to activate SIRT1 in NAD⁺ independent manners [38,39]. The cAMP not only directly interacts with its receptor protein but also activates the downstream protein kinases to control gene transcription [45]. We herein found that PKA instead of EPAC was required for SIRT1 activation by METRNL. Gerhart-Hines et al. found that PKA phosphorylated SIRT1 on the highly conserved serine 434 residue to increase the intrinsic enzymatic activity [38]. Besides, cAMP/PKA activation also promoted the dissociation of SIRT1 from its endogenous inhibitor [39]. The cAMP responsive element binding protein serves as a critical transcription factor in cAMP/PKA signaling axis and is recruited to SIRT1 chromatin to directly promote SIRT1 expression [46]. This might partially explain the observation of an increased SIRT1 expression after METRNL overexpression. EPAC is also an effector of cAMP pathway and our previous data found that cAMP-dependent EPAC activation was sufficient to relieve oxidative stress and apoptosis in hearts upon hyperglycemic or septic stimulation [30, 47]. However, SIRT1 activation and the beneficial effects were

preserved in METRNL-overexpressed cells with *siEpac* transfection.

Considering the translational value of the present findings, the combined effects of METRNL and DOX on tumor growth were also measured *in vivo* and *in vitro*. The results implied that METRNL was capable of reducing DOX-induced cardiotoxicity but preserving its antitumor potency. Previous studies determined that the same molecule or intervention may cause different, or even diametrically opposite, impacts in different cell types or disease models [48–50]. Besides, the biological identities vary enormously from the cancer cells to mammalian cardiomyocytes, such as the proliferative capacity and metabolic status, etc. Particularly, the membranous components of cancer cells are reported to be different from that in noncancerous cells; therefore, further studies are needed to determine whether the METRNL receptor disappears or a specific receptor exists on the surface of cancer cells, including the 4T1 cells [51,52]. Of note, we tested only in one cancer cell line, and it is unclear whether the preservation of tumor-killing capacity by DOX could extend to all malignant cell types.

In summary, we determine a robust expression and secretion of METRNL from the heart and cardiomyocytes that are decreased by DOX treatment. Besides, METRNL activates SIRT1 via cAMP/PKA signaling axis to prevent DOX-elicited oxidative stress, apoptosis and cardiac dysfunction in an autocrine manner. More importantly, METRNL does not affect the tumor-killing capacity of DOX. Yet, the precise receptor of METRNL remains unclear and desperately need further investigation. Based on this findings, we speculate that METRNL is required for a healthy microenvironment to decrease oxidative damage and apoptosis in DOX-treated hearts, thereby serving as a promising therapeutic target to overcome DOX-induced cardiotoxicity.

Funding

This work was supported by grants from National Natural Science Foundation of China (81470516, 81700254), the Key Project of the National Natural Science Foundation (81530012), National Key R&D Program of China (2018YFC1311300), the Fundamental Research Funds for the Central Universities (2042017kf0085, 2042018kf1032), Development Center for Medical Science and Technology National Health and Family Planning Commission of the People's Republic of China (The prevention and control project of cardiovascular disease, 2016ZX-008-01) and Science and Technology Planning Projects of Wuhan (2018061005132295).

Declaration of competing interest

None declared.

Acknowledgements

We thank Dr. Q Yang in the Department of Breast and Thyroid Surgery, Renmin Hospital of Wuhan University for the 4T1 cells. We are also grateful to Dr. X Gao in the Model Animal Research Center of Nanjing University for kindly providing the *Sirt1* conditional floxed mice.

Appendix A. Supplementary data

Supplementary data to this article can be found online at <https://doi.org/10.1016/j.redox.2020.101747>.

References

- [1] S.H. Armenian, C. Lacchetti, A. Barac, J. Carver, L.S. Constine, N. Denduluri, et al., Prevention and monitoring of cardiac dysfunction in survivors of adult cancers: American society of clinical oncology clinical practice guideline, *J. Clin. Oncol.* 35 (2017) 893–911.
- [2] K.B. Wallace, V.A. Sardao, P.J. Oliveira, Mitochondrial determinants of doxorubicin-induced cardiomyopathy, *Circ. Res.* 126 (2020) 926–941.
- [3] J.H. Doroshow, G.Y. Locker, C.E. Myers, Enzymatic defenses of the mouse heart against reactive oxygen metabolites: alterations produced by doxorubicin, *J. Clin. Invest.* 65 (1980) 128–135.
- [4] X. Zhang, C. Hu, C.Y. Kong, P. Song, H.M. Wu, S.C. Xu, et al., FNDC5 alleviates oxidative stress and cardiomyocyte apoptosis in doxorubicin-induced cardiotoxicity via activating AKT, *Cell Death Differ.* 27 (2020) 540–555.
- [5] C. Hu, X. Zhang, W. Wei, N. Zhang, H. Wu, Z. Ma, et al., Matrine attenuates oxidative stress and cardiomyocyte apoptosis in doxorubicin-induced cardiotoxicity via maintaining AMPKalpha/UCP2 pathway, *Acta Pharm. Sin. B* 9 (2019) 690–701.
- [6] C. Hu, X. Zhang, N. Zhang, W.Y. Wei, L.L. Li, Z.G. Ma, et al., Osteocrin attenuates inflammation, oxidative stress, apoptosis, and cardiac dysfunction in doxorubicin-induced cardiotoxicity, *Clin. Transl. Med.* 10 (2020) e124.
- [7] X. Zhang, J.X. Zhu, Z.G. Ma, H.M. Wu, S.C. Xu, P. Song, et al., Rosmarinic acid alleviates cardiomyocyte apoptosis via cardiac fibroblast in doxorubicin-induced cardiotoxicity, *Int. J. Biol. Sci.* 15 (2019) 556–567.
- [8] Y.P. Yuan, Z.G. Ma, X. Zhang, S.C. Xu, X.F. Zeng, Z. Yang, et al., CTRP3 protected against doxorubicin-induced cardiac dysfunction, inflammation and cell death via activation of Sirt1, *J. Mol. Cell. Cardiol.* 114 (2018) 38–47.
- [9] M. Russo, F. Guida, L. Paparo, G. Trinchese, R. Aitoro, C. Avagliano, et al., The novel butyrate derivative phenylalanine-butylamide protects from doxorubicin-induced cardiotoxicity, *Eur. J. Heart Fail.* 21 (2019) 519–528.
- [10] S.E. Lipschultz, R.E. Scully, S.R. Lipsitz, S.E. Sallan, L.B. Silverman, T.L. Miller, et al., Assessment of dexrazoxane as a cardioprotectant in doxorubicin-treated children with high-risk acute lymphoblastic leukaemia: long-term follow-up of a prospective, randomised, multicentre trial, *Lancet Oncol.* 11 (2010) 950–961.
- [11] J.M. Scott, A. Khakoo, J.R. Mackey, M.J. Haykowsky, P.S. Douglas, L.W. Jones, Modulation of anthracycline-induced cardiotoxicity by aerobic exercise in breast cancer: current evidence and underlying mechanisms, *Circulation* 124 (2011) 642–650.
- [12] A. Ascensao, J. Lumini-Oliveira, N.G. Machado, R.M. Ferreira, I.O. Goncalves, A. C. Moreira, et al., Acute exercise protects against calcium-induced cardiac mitochondrial permeability transition pore opening in doxorubicin-treated rats, *Clin. Sci. (Lond.)* 120 (2011) 37–49.
- [13] B.T. Jensen, C.Y. Lien, D.S. Hydock, C.M. Schneider, R. Hayward, Exercise mitigates cardiac doxorubicin accumulation and preserves function in the rat, *J. Cardiovasc. Pharmacol.* 62 (2013) 263–269.
- [14] T.L. Parry, R. Hayward, Exercise training does not affect anthracycline antitumor efficacy while attenuating cardiac dysfunction, *Am. J. Physiol. Regul. Integr. Comp. Physiol.* 309 (2015) R675–R683.
- [15] J.M. Scott, T.S. Nilsen, D. Gupta, L.W. Jones, Exercise therapy and cardiovascular toxicity in cancer, *Circulation* 137 (2018) 1176–1191.
- [16] L.W. Jones, N.D. Eves, M. Haykowsky, S.J. Freedland, J.R. Mackey, Exercise intolerance in cancer and the role of exercise therapy to reverse dysfunction, *Lancet Oncol.* 10 (2009) 598–605.
- [17] M. Whitham, M.A. Febbraio, The ever-expanding myokine: discovery challenges and therapeutic implications, *Nat. Rev. Drug Discov.* 15 (2016) 719–729.
- [18] N. Otaka, R. Shibata, K. Ohashi, Y. Uemura, T. Kambara, T. Enomoto, et al., Myonectin is an exercise-induced myokine that protects the heart from ischemia-reperfusion injury, *Circ. Res.* 123 (2018) 1326–1338.
- [19] S. Wang, Y. Wang, Z. Zhang, Q. Liu, J. Gu, Cardioprotective effects of fibroblast growth factor 21 against doxorubicin-induced toxicity via the SIRT1/LKB1/AMPK pathway, *Cell Death Dis.* 8 (2017), e3018.
- [20] K. Suzuki, B. Murtuza, N. Suzuki, R.T. Smolenski, M.H. Yacoub, Intracoronary infusion of skeletal myoblasts improves cardiac function in doxorubicin-induced heart failure, *Circulation* 104 (2001) I213–I217.
- [21] R.R. Rao, J.Z. Long, J.P. White, K.J. Svensson, J. Lou, I. Lokurkar, et al., Meteorin-like is a hormone that regulates immune-adipose interactions to increase beige fat thermogenesis, *Cell* 157 (2014) 1279–1291.
- [22] Z.Y. Li, J. Song, S.L. Zheng, M.B. Fan, Y.F. Guan, Y. Qu, et al., Adipocyte Metrn antagonizes insulin resistance through PPARgamma signaling, *Diabetes* 64 (2015) 4011–4022.
- [23] G.S. Baht, A. Bareja, D.E. Lee, R.R. Rao, R. Huang, J.L. Huebner, et al., Meteorin-like facilitates skeletal muscle repair through a Stat 3/IGF-1 mechanism, *Nat Metab* 2 (2020) 278–289.
- [24] Z.X. Liu, H.H. Ji, M.P. Yao, L. Wang, Y. Wang, P. Zhou, et al., Serum Metrn is associated with the presence and severity of coronary artery disease, *J. Cell Mol. Med.* 23 (2019) 271–280.
- [25] L. Xu, Y. Cai, Y. Wang, C. Xu, Meteorin-like (METRNL) attenuates myocardial ischemia/reperfusion injury-induced cardiomyocytes apoptosis by alleviating endoplasmic reticulum stress via activation of AMPK-PAK2 signaling in H9C2 cells, *Med. Sci. Mon. Int. Med. J. Exp. Clin. Res.* 26 (2020), e924564.
- [26] Z.G. Ma, Y.P. Yuan, X. Zhang, S.C. Xu, C.Y. Kong, P. Song, et al., C1q-tumour necrosis factor-related protein-3 exacerbates cardiac hypertrophy in mice, *Cardiovasc. Res.* 115 (2019) 1067–1077.
- [27] X. Zhang, Z.G. Ma, Y.P. Yuan, S.C. Xu, W.Y. Wei, P. Song, et al., Rosmarinic acid attenuates cardiac fibrosis following long-term pressure overload via AMPKalpha/Smad 3 signaling, *Cell Death Dis.* 9 (2018) 102.
- [28] Z.G. Ma, J. Dai, Y.P. Yuan, Z.Y. Bian, S.C. Xu, Y.G. Jin, et al., T-bet deficiency attenuates cardiac remodelling in rats, *Basic Res. Cardiol.* 113 (2018) 19.
- [29] H.K. Wu, Y. Zhang, C.M. Cao, X. Hu, M. Fang, Y. Yao, et al., Glucose-sensitive myokine/cardiokine MG53 regulates systemic insulin response and metabolic homeostasis, *Circulation* 139 (2019) 901–914.
- [30] Z.G. Ma, Y.P. Yuan, S.C. Xu, W.Y. Wei, C.R. Xu, X. Zhang, et al., CTRP3 attenuates cardiac dysfunction, inflammation, oxidative stress and cell death in diabetic cardiomyopathy in rats, *Diabetologia* 60 (2017) 1126–1137.

- [31] Q.Q. Wu, C. Liu, Z. Cai, Q. Xie, T. Hu, M. Duan, et al., High-mobility group AT-hook 1 promotes cardiac dysfunction in diabetic cardiomyopathy via autophagy inhibition, *Cell Death Dis.* 11 (2020) 160.
- [32] X. Zhang, C. Hu, N. Zhang, W.Y. Wei, L.L. Li, H.M. Wu, et al., Matrine attenuates pathological cardiac fibrosis via RPS5/p38 in mice, *Acta Pharmacol. Sin.* (2020).
- [33] P. Pacher, L. Liaudet, P. Bai, J.G. Mabley, P.M. Kaminski, L. Virag, et al., Potent metalloporphyrin peroxynitrite decomposition catalyst protects against the development of doxorubicin-induced cardiac dysfunction, *Circulation* 107 (2003) 896–904.
- [34] M. Yamamoto, T.W. Kensler, H. Motohashi, The KEAP1-NRF2 system: a thiol-based sensor-effector apparatus for maintaining redox homeostasis, *Physiol. Rev.* 98 (2018) 1169–1203.
- [35] M. Rasanen, J. Degerman, T.A. Nissinen, I. Miinalainen, R. Kerkela, A. Siltanen, et al., VEGF-B gene therapy inhibits doxorubicin-induced cardiotoxicity by endothelial protection, *Proc. Natl. Acad. Sci. U. S. A.* 113 (2016) 13144–13149.
- [36] L. Lai, L. Yan, S. Gao, C.L. Hu, H. Ge, A. Davidow, et al., Type 5 adenylyl cyclase increases oxidative stress by transcriptional regulation of manganese superoxide dismutase via the SIRT1/FoxO3a pathway, *Circulation* 127 (2013) 1692–1701.
- [37] C.P. Hsu, P. Zhai, T. Yamamoto, Y. Maejima, S. Matsushima, N. Hariharan, et al., Silent information regulator 1 protects the heart from ischemia/reperfusion, *Circulation* 122 (2010) 2170–2182.
- [38] Z. Gerhart-Hines, J.J. Dominy, S.M. Blattler, M.P. Jedrychowski, A.S. Banks, J. H. Lim, et al., The cAMP/PKA pathway rapidly activates SIRT1 to promote fatty acid oxidation independently of changes in NAD(+), *Mol. Cell.* 44 (2011) 851–863.
- [39] V. Nin, C. Escande, C.C. Chini, S. Giri, J. Camacho-Pereira, J. Matalonga, et al., Role of deleted in breast cancer 1 (DBC1) protein in SIRT1 deacetylase activation induced by protein kinase A and AMP-activated protein kinase, *J. Biol. Chem.* 287 (2012) 23489–23501.
- [40] J.P. Kitt, D.A. Bryce, S.D. Minter, J.M. Harris, Raman spectroscopy reveals selective interactions of cytochrome c with cardiolipin that correlate with membrane permeability, *J. Am. Chem. Soc.* 139 (2017) 3851–3860.
- [41] Y. Ichikawa, M. Ghanefar, M. Bayeva, R. Wu, A. Khechaduri, P.S. Naga, et al., Cardiotoxicity of doxorubicin is mediated through mitochondrial iron accumulation, *J. Clin. Invest.* 124 (2014) 617–630.
- [42] D. Herranz, M. Serrano, SIRT1: recent lessons from mouse models, *Nat. Rev. Canc.* 10 (2010) 819–823.
- [43] S. Matsui, T. Sasaki, D. Kohno, K. Yaku, A. Inutsuka, H. Yokota-Hashimoto, et al., Neuronal SIRT1 regulates macronutrient-based diet selection through FGF21 and oxytocin signalling in mice, *Nat. Commun.* 9 (2018) 4604.
- [44] C. Zhang, Y. Feng, S. Qu, X. Wei, H. Zhu, Q. Luo, et al., Resveratrol attenuates doxorubicin-induced cardiomyocyte apoptosis in mice through SIRT1-mediated deacetylation of p53, *Cardiovasc. Res.* 90 (2011) 538–545.
- [45] M. Crasnier-Mednansky, Is there any role for cAMP-CRP in carbon catabolite repression of the *Escherichia coli* lac operon? *Nat. Rev. Microbiol.* 6 (2008) 954, 954.
- [46] S. Fusco, C. Ripoli, M.V. Podda, S.C. Ranieri, L. Leone, G. Toietta, et al., A role for neuronal cAMP responsive-element binding (CREB)-1 in brain responses to calorie restriction, *Proc. Natl. Acad. Sci. U. S. A.* 109 (2012) 621–626.
- [47] P. Song, D.F. Shen, Y.Y. Meng, C.Y. Kong, X. Zhang, Y.P. Yuan, et al., Geniposide protects against sepsis-induced myocardial dysfunction through AMPK α -dependent pathway, *Free Radic. Biol. Med.* 152 (2020) 186–196.
- [48] Y. Sassi, A. Ahles, D.J. Truong, Y. Baqi, S.Y. Lee, B. Husse, et al., Cardiac myocyte-secreted cAMP exerts paracrine action via adenosine receptor activation, *J. Clin. Invest.* 124 (2014) 5385–5397.
- [49] M. Appari, A. Breitbart, F. Brandes, M. Szaroszyk, N. Froese, M. Korf-Klingebiel, et al., C1q-TNF-Related protein-9 promotes cardiac hypertrophy and failure, *Circ. Res.* 120 (2017) 66–77.
- [50] Y. Sun, W. Yi, Y. Yuan, W.B. Lau, D. Yi, X. Wang, et al., C1q/tumor necrosis factor-related protein-9, a novel adipocyte-derived cytokine, attenuates adverse remodeling in the ischemic mouse heart via protein kinase A activation, *Circulation* 128 (2013) S113–S120.
- [51] A. Erazo-Oliveras, N.R. Fuentes, R.C. Wright, R.S. Chapkin, Functional link between plasma membrane spatiotemporal dynamics, cancer biology, and dietary membrane-altering agents, *Canc. Metastasis Rev.* 37 (2018) 519–544.
- [52] J. Bi, T.A. Ichu, C. Zanca, H. Yang, W. Zhang, Y. Gu, et al., Oncogene amplification in growth factor signaling pathways renders cancers dependent on membrane lipid remodeling, *Cell Metabol.* 30 (2019) 525–538.